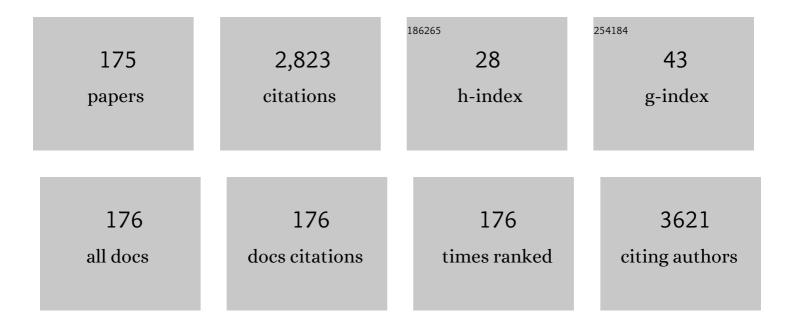
Sebastião W Da Silva

List of Publications by Year in descending order

Source: https://exaly.com/author-pdf/9328340/publications.pdf

Version: 2024-02-01



#	Article	IF	CITATIONS
1	Size controlling and tailoring the properties of Gd Zn1-O nanoparticles. Ceramics International, 2022, 48, 4324-4331.	4.8	3
2	Detection of SARS-CoV-2 virus via dynamic light scattering using antibody-gold nanoparticle bioconjugates against viral spike protein. Talanta, 2022, 243, 123355.	5.5	16
3	Tuning intrinsic defects in ZnO films by controlling the vacuum annealing temperature: an experimental and theoretical approach. Physica Scripta, 2022, 97, 075811.	2.5	1
4	Oral delivery of fish oil in oil-in-water nanoemulsion: development, colloidal stability and modulatory effect on in vivo inflammatory induction in mice. Biomedicine and Pharmacotherapy, 2021, 133, 110980.	5.6	18
5	Charge localization and hopping in a topologically engineered graphene nanoribbon. Scientific Reports, 2021, 11, 5142.	3.3	5
6	Fe content effects on structural, electrical and magnetic properties of Fe-doped ITO polycrystalline powders. Journal of Alloys and Compounds, 2021, 867, 158866.	5.5	7
7	Core-shell Au/Fe3O4 nanocomposite synthesized by thermal decomposition method: Structural, optical, and magnetic properties. Applied Surface Science, 2021, 563, 150290.	6.1	10
8	Structural, optical and magnetic properties of CoAl Fe2-O4 nanoparticles prepared by combustion reaction method. Journal of Alloys and Compounds, 2021, 887, 161398.	5.5	6
9	PEGlatyon-SPION surface functionalization with folic acid for magnetic hyperthermia applications. Materials Research Express, 2020, 7, 015078.	1.6	24
10	A comprehensive study on the effects of gamma radiation on the physical properties of a two-dimensional WS ₂ monolayer semiconductor. Nanoscale Horizons, 2020, 5, 259-267.	8.0	26
11	Charge Transport Mechanism in Chevron-Graphene Nanoribbons. Journal of Physical Chemistry C, 2020, 124, 22392-22398.	3.1	3
12	Field-driven spin reorientation in SmMnO3 polycrystalline powders. Journal of Alloys and Compounds, 2020, 845, 156327.	5.5	6
13	Embedding CoPt magnetic nanoparticles within a phosphate glass matrix. Journal of Alloys and Compounds, 2020, 848, 156576.	5.5	5
14	Smooth gap tuning strategy for cove-type graphene nanoribbons. RSC Advances, 2020, 10, 26937-26943.	3.6	10
15	The influence of NLC composition on curcumin loading under a physicochemical perspective and in vitro evaluation. Colloids and Surfaces A: Physicochemical and Engineering Aspects, 2020, 602, 125070.	4.7	29
16	Transport of quasiparticles in coronene-based graphene nanoribbons. Journal of Materials Chemistry C, 2020, 8, 12100-12107.	5.5	8
17	Cation distribution of Zn Co1-Fe2O4 nanoparticles: A resonant X-ray diffraction study. Journal of Alloys and Compounds, 2020, 842, 155751.	5.5	10
18	Tailoring the physical and chemical properties of Sn _{1â^'x} Co _x O ₂ nanoparticles: an experimental and theoretical approach. Physical Chemistry Chemical Physics, 2020, 22, 3702-3714.	2.8	19

SebastiãO W DA Silva

#	Article	IF	CITATIONS
19	Nanoemulsion-based systems as a promising approach for enhancing the antitumoral activity of pequi oil (Caryocar brasilense Cambess.) in breast cancer cells. Journal of Drug Delivery Science and Technology, 2020, 58, 101819.	3.0	12
20	Lattice strain effects on the structural properties and band gap tailoring in columnarly grown Fe-doped SnO ₂ films deposited by DC sputtering. Journal Physics D: Applied Physics, 2019, 52, 465306.	2.8	5
21	Defective graphene domains in boron nitride sheets. Journal of Molecular Modeling, 2019, 25, 230.	1.8	6
22	Stability conditions of armchair graphene nanoribbon bipolarons. Journal of Molecular Modeling, 2019, 25, 245.	1.8	8
23	Polaron properties in 2D organic molecular crystals: directional dependence of non-local electron–phonon coupling. Journal of Molecular Modeling, 2019, 25, 149.	1.8	2
24	Same Charge Polaron and Bipolaron Scattering on Conducting Polymers. Journal of Physical Chemistry A, 2019, 123, 1319-1327.	2.5	8
25	Surfaceâ€enhanced Raman spectroscopy for successful probing of itraconazole within poly(lacticâ€ <i>co</i> â€glycolic acid) nanoparticles. Journal of Raman Spectroscopy, 2019, 50, 1085-1093.	2.5	1
26	Tuning the electronic structure properties of MoS ₂ monolayers with carbon doping. Physical Chemistry Chemical Physics, 2019, 21, 11168-11174.	2.8	10
27	Stationary and Dynamical Properties of Polarons in Anisotropic C ₆₀ -Crystals. Journal of Physical Chemistry C, 2019, 123, 13410-13418.	3.1	7
28	Fast predictions of exciton diffusion length in organic materials. Journal of Materials Chemistry C, 2019, 7, 4066-4071.	5.5	13
29	Bipolaron Dynamics in Graphene Nanoribbons. Scientific Reports, 2019, 9, 2909.	3.3	14
30	Modeling Polaron Diffusion in Oligoacene-like Crystals. Journal of Physical Chemistry C, 2019, 123, 4715-4720.	3.1	9
31	Dynamical Mechanism of Polarons and Bipolarons in Poly(p-Phenylene Vinylene). Scientific Reports, 2019, 9, 18131.	3.3	3
32	Effective Mass of Quasiparticles in Armchair Graphene Nanoribbons. Scientific Reports, 2019, 9, 17990.	3.3	5
33	In vivo toxicological evaluation of polymer brush engineered nanoceria: impact of brush charge. Nanotoxicology, 2019, 13, 305-325.	3.0	3
34	Quasiparticle description of transition metal dichalcogenide nanoribbons. Physical Review B, 2019, 99,	3.2	8
35	Evidence of surface spin-glass behavior in NiFe2O4 nanoparticles determined using magnetic resonance technique. Journal of Magnetism and Magnetic Materials, 2019, 476, 392-397.	2.3	14
36	Mössbauer spectroscopy control of the preparation of citric- and mandelic acid functionalized nanomagnetites. Hyperfine Interactions, 2018, 239, 1.	0.5	2

#	Article	IF	CITATIONS
37	Spin-Orbit Effects on the Dynamical Properties of Polarons in Graphene Nanoribbons. Scientific Reports, 2018, 8, 1914.	3.3	8
38	Charge Carrier Scattering in Polymers: A New Neutral Coupled Soliton Channel. Scientific Reports, 2018, 8, 6595.	3.3	5
39	Fabrication and characterization of glycine-loaded PEG nanoparticles for drug delivering: A comprehensive SERS study. Applied Surface Science, 2018, 450, 396-403.	6.1	9
40	Dynamic Formation of Bipolaron–Exciton Complexes in Conducting Polymers. Journal of Physical Chemistry A, 2018, 122, 3866-3872.	2.5	1
41	Plasmonic-excitonic multi-hybrid glass-based nanocomposites incorporating Ag plus core-shell CdSe/CdS and alloyed CdSxSe1â~x nanoparticles. Ceramics International, 2018, 44, 208-215.	4.8	2
42	Polyethyleneglycol nanoparticles adsorbed to glycine as a bioengineered neomaterial for application in inflammatory processes. International Journal of Advanced Engineering Research and Science, 2018, 5, 10-16.	0.1	0
43	Optical and magnetic properties of Co-doped ZnO nanoparticles and the onset of ferromagnetic order. Journal of Applied Physics, 2017, 121, .	2.5	24
44	Electron–phonon coupling effects on intrachain polaron recombination in conjugated polymers. Journal of Molecular Modeling, 2017, 23, 42.	1.8	2
45	Mössbauer and Raman spectroscopic study of oxidation and reduction of iron oxide nanoparticles promoted by various carboxylic acid layers. Journal of Radioanalytical and Nuclear Chemistry, 2017, 312, 111-119.	1.5	7
46	Polaron and bipolaron stability on paraphenylene polymers. Journal of Molecular Modeling, 2017, 23, 59.	1.8	4
47	Maghemite–gold core–shell nanostructures (γ-Fe2O3@Au) surface-functionalized with aluminium phthalocyanine for multi-task imaging and therapy. RSC Advances, 2017, 7, 11223-11232.	3.6	16
48	Characterization of polycrystalline SnO2 films deposited by DC sputtering technique with potential for technological applications. Journal of the European Ceramic Society, 2017, 37, 3375-3380.	5.7	16
49	Bloch oscillations in organic and inorganic polymers. Journal of Chemical Physics, 2017, 146, 144903.	3.0	3
50	Effect of Co co-doping on the optical properties of ZnTe:Mn nanocrystals. Physical Chemistry Chemical Physics, 2017, 19, 1158-1166.	2.8	11
51	Bond length pattern associated with charge carriers in armchair graphene nanoribbons. Journal of Molecular Modeling, 2017, 23, 293.	1.8	9
52	Magnetic nanohydrogel obtained by miniemulsion polymerization of poly(acrylic acid) grafted onto derivatized dextran. Carbohydrate Polymers, 2017, 178, 378-385.	10.2	11
53	SERS Investigation of Cancer Cells Treated with PDT: Quantification of Cell Survival and Follow-up. Scientific Reports, 2017, 7, 7175.	3.3	25
54	Zirconia‣upported Cobalt Catalysts: Activity and Selectivity in NO Reduction by CO. ChemistrySelect, 2017, 2, 11565-11573.	1.5	4

#	Article	IF	CITATIONS
55	Nanocapsules for the co-delivery of selol and doxorubicin to breast adenocarcinoma 4T1 cells in vitro. Artificial Cells, Nanomedicine and Biotechnology, 2017, 46, 1-11.	2.8	10
56	Fe-doping effects on the structural, vibrational, magnetic, and electronic properties of ceria nanoparticles. Journal of Applied Physics, 2017, 122, .	2.5	19
57	Gadolinium ferrite nanoparticles: Synthesis and morphological, structural and magnetic properties. Ceramics International, 2017, 43, 4042-4047.	4.8	21
58	Investigation of additional Raman modes in ZnO and Eu0.01Zn0.99O nanoparticles synthesized by the solution combustion method. Journal of Alloys and Compounds, 2017, 691, 416-421.	5.5	12
59	Effect of the thickness reduction on the structural, surface and magnetic properties of α-Fe2O3 thin films. Thin Solid Films, 2016, 607, 50-54.	1.8	32
60	Solubility limit of Mn2+ ions in Zn1â^'x Mn x Te nanocrystals grown within an ultraviolet-transparent glass template. Journal of Nanoparticle Research, 2016, 18, 1.	1.9	8
61	Low-Temperature Seebeck Coefficients for Polaron-Driven Thermoelectric Effect in Organic Polymers. Journal of Physical Chemistry A, 2016, 120, 4923-4927.	2.5	7
62	Impact of the Electron–Phonon Interactions on the Polaron Dynamics in Graphene Nanoribbons. Journal of Physical Chemistry A, 2016, 120, 4901-4906.	2.5	19
63	Fine structure of gold nanoparticles stabilized by buthyldithiol: Species identified by Mössbauer spectroscopy. Colloids and Surfaces A: Physicochemical and Engineering Aspects, 2016, 504, 260-266.	4.7	9
64	Evidence of competition in the incorporation of Co2+and Mn2+ions into the structure of ZnTe nanocrystals. RSC Advances, 2016, 6, 101226-101234.	3.6	7
65	Aluminium-phthalocyanine chloride nanoemulsions for anticancer photodynamic therapy: Development and in vitro activity against monolayers and spheroids of human mammary adenocarcinoma MCF-7 cells. Journal of Nanobiotechnology, 2015, 13, 36.	9.1	70
66	Rifampicin adsorbed onto magnetite nanoparticle: SERS study and insight on the molecular arrangement and light effect. Journal of Raman Spectroscopy, 2015, 46, 765-771.	2.5	7
67	Evolution of the doping regimes in the Al-doped SnO ₂ nanoparticles prepared by a polymer precursor method. Journal of Physics Condensed Matter, 2015, 27, 095301.	1.8	44
68	Transport of Polarons in Graphene Nanoribbons. Journal of Physical Chemistry Letters, 2015, 6, 510-514.	4.6	41
69	Structural and magnetic properties of ZnO–CoFe2O4 nanocomposites. Journal of Magnetism and Magnetic Materials, 2015, 389, 27-33.	2.3	30
70	Limit of Exciton Diffusion in Highly Ordered π-Conjugated Systems. Journal of Physical Chemistry C, 2015, 119, 19654-19659.	3.1	10
71	Thermal-annealing effects on the structural and magnetic properties of 10% Fe-doped SnO2 nanoparticles synthetized by a polymer precursor method. Journal of Magnetism and Magnetic Materials, 2015, 375, 74-79.	2.3	9
72	Doping effects on the structural, magnetic, and hyperfine properties of Gd-doped SnO2 nanoparticles. Journal of Nanoparticle Research, 2014, 16, 1.	1.9	10

#	Article	IF	CITATIONS
73	Characterization of tetraethylene glycol passivated iron nanoparticles. Applied Surface Science, 2014, 315, 337-345.	6.1	10
74	Reactive Scattering between Excitons and Charge Carriers in Conjugated Polymers. Journal of Physical Chemistry C, 2014, 118, 23451-23458.	3.1	13
75	Shell Thickness Modulation in Ultrasmall CdSe/CdS _{<i>x</i>} Se _{1–<i>x</i>} /CdS Core/Shell Quantum Dots <i>via</i> 1-Thioglycerol. ACS Nano, 2014, 8, 1913-1922.	14.6	53
76	Carbon dioxide adsorption on doped boron nitride nanotubes. RSC Advances, 2014, 4, 28249-28258.	3.6	34
77	PEGylation of SPIONs by polycondensation reactions: a new strategy to improve colloidal stability in biological media. Journal of Nanoparticle Research, 2013, 15, 1.	1.9	14
78	Experimental evidences of substitutional solution of Er dopant in Er-doped SnO2 nanoparticles. Journal of Nanoparticle Research, 2013, 15, 1.	1.9	13
79	Influence of bipolaron density on the transport properties of thermalized organic conductors. International Journal of Quantum Chemistry, 2013, 113, 2540-2545.	2.0	2
80	An extensive investigation of reactions involved in the nitrogen trifluoride dissociation. New Journal of Chemistry, 2013, 37, 3244.	2.8	1
81	Effects of temperature and electric field induced phase transitions on the dynamics of polarons and bipolarons. New Journal of Chemistry, 2013, 37, 2829.	2.8	48
82	Multiphonon Raman Scattering in Coupled Cd _{1–<i>x</i>} Mn _{<i>x</i>} S Nanoparticles: Magnetic Doping and Thermal Annealing. Journal of Physical Chemistry C, 2013, 117, 657-662.	3.1	19
83	Modified Phonon Confinement Model and Its Application to CdSe/CdS Core–Shell Magic-Sized Quantum Dots Synthesized in Aqueous Solution by a New Route. Journal of Physical Chemistry C, 2013, 117, 1904-1914.	3.1	48
84	Raman spectroscopy of very small Cd _{1â^'x} Co _x S quantum dots grown by a novel protocol: direct observation of acousticâ€optical phonon coupling. Journal of Raman Spectroscopy, 2013, 44, 1022-1032.	2.5	26
85	SERS as a valuable tool for detection and treatment followâ€up of fungal infection in mice lungs: use of Amphotericin B and its nanoencapsulation onto magnetic nanoparticles. Journal of Raman Spectroscopy, 2013, 44, 695-702.	2.5	12
86	GISAXS study on the annealing behavior of sputtered HfO2 thin films. Materials Research Society Symposia Proceedings, 2013, 1528, 1.	0.1	0
87	Temperature-dependent Raman study of thermal parameters in CdS quantum dots. Nanotechnology, 2012, 23, 125701.	2.6	34
88	Dilute magnetism in Zn1â^'xMnxTe nanocrystals grown in a glass template. Chemical Physics Letters, 2012, 541, 44-48.	2.6	22
89	Phase transition in sputtered HfO <inf>2</inf> thin films: A qualitative raman study. , 2012, , .		0
90	Phase transition in sputtered HfO2 thin films: A qualitative Raman study. Applied Surface Science, 2012, 261, 727-729.	6.1	14

#	Article	IF	CITATIONS
91	Anti-CEA loaded maghemite nanoparticles as a theragnostic device for colorectal cancer. International Journal of Nanomedicine, 2012, 7, 5271.	6.7	27
92	Raman study of cations' distribution in Zn x Mg1â^'x Fe2O4 nanoparticles. Journal of Nanoparticle Research, 2012, 14, 1.	1.9	78
93	Sol–gel synthesis of silica–cobalt composites by employing Co3O4 colloidal dispersions. Colloids and Surfaces A: Physicochemical and Engineering Aspects, 2012, 395, 217-224.	4.7	34
94	SERRS Study of Molecular Arrangement of Amphotericin B Adsorbed onto Iron Oxide Nanoparticles Precoated with a Bilayer of Lauric Acid. Journal of Physical Chemistry C, 2011, 115, 20442-20448.	3.1	21
95	Effect of Fe2O3 concentration on the structure of the SiO2–Na2O–Al2O3–B2O3 glass system. Spectrochimica Acta - Part A: Molecular and Biomolecular Spectroscopy, 2011, 81, 140-143.	3.9	69
96	<i>>H</i> ₂ ⁺ dynamical properties in the electronic states 7 <i>j</i> Ïf, 8 <i>j</i> Ïf, 8 <i>k</i> Ïf, 7 <i>i</i> I, and 8 <i>j</i> p. International Journal of Quantum Chemistry, 2011, 111, 1316-1320.	2.0	2
97	Evidences of the evolution from solid solution to surface segregation in Niâ€doped SnO ₂ nanoparticles using Raman spectroscopy. Journal of Raman Spectroscopy, 2011, 42, 1081-1086.	2.5	72
98	Resonant Raman scattering in CdS _{<i>x</i>} Se _{1â^'<i>x</i>} nanocrystals: effects of phonon confinement, composition, and elastic strain. Journal of Raman Spectroscopy, 2011, 42, 1660-1669.	2.5	37
99	Confirming the lattice contraction in CdSe nanocrystals grown in a glass matrix by Raman scattering. Journal of Raman Spectroscopy, 2010, 41, 1302-1305.	2.5	35
100	ZnTe nanocrystal formation and growth control on UV-transparent substrate. Chemical Physics Letters, 2010, 500, 46-48.	2.6	23
101	Thermal rate coefficients calculation for the H ⁺ + LiH reaction. International Journal of Quantum Chemistry, 2010, 110, 2024-2028.	2.0	5
102	Effect of the Zn content in the structural and magnetic properties of ZnxMg1â^'xFe2O4 mixed ferrites monitored by Raman and Mössbauer spectroscopies. Journal of Applied Physics, 2010, 107, .	2.5	40
103	Influence of the Mg-content on the cation distribution in cubic Mg Fe3O4 nanoparticles. Journal of Solid State Chemistry, 2009, 182, 2423-2429.	2.9	109
104	Interchain interaction effects on polaron–bipolaron transition on conducting polymers. Journal of Materials Science, 2008, 43, 585-590.	3.7	5
105	Chain length effects on nonlinear excitation transitions in transâ€polyacetylene. International Journal of Quantum Chemistry, 2008, 108, 2507-2511.	2.0	2
106	Dynamics of photoexcitations with interchain coupling in conjugated polymers. International Journal of Quantum Chemistry, 2008, 108, 2442-2447.	2.0	3
107	Electric field effects on the spatial energy transport in self-assembled quantum dots. Journal Physics D: Applied Physics, 2008, 41, 105104.	2.8	1
108	Effects of high-temperature annealing on the optical phonons and nitrogen local vibrational modes in GaAs1â^'xNx epilayers. Applied Physics Letters, 2008, 93, 252105.	3.3	1

#	Article	IF	CITATIONS
109	Influence of the optical control in the lateral transport of carriers in InGaAsâ^•GaAs one-side modulation-doped quantum wells. Journal of Applied Physics, 2007, 102, .	2.5	2
110	The thermal stability of maghemite-silica nanocomposites: An investigation using X-ray diffraction and Raman spectroscopy. Journal of Alloys and Compounds, 2007, 434-435, 650-654.	5.5	44
111	The influence of cobalt population on the structural properties of CoxFe3â^'xO4. Journal of Applied Physics, 2007, 101, 09M514.	2.5	81
112	Aging Investigation of Cobalt Ferrite Nanoparticles in Low pH Magnetic Fluid. Langmuir, 2007, 23, 9611-9617.	3.5	91
113	Study of molecular surface coating on the stability of maghemite nanoparticles. Surface Science, 2007, 601, 3921-3925.	1.9	59
114	Raman spectroscopy of cobalt ferrite nanocomposite in silica matrix prepared by sol–gel method. Journal of Non-Crystalline Solids, 2006, 352, 1602-1606.	3.1	36
115	Effects of impurities on polaron dynamics in conjugated polymers: Effective potentials. International Journal of Quantum Chemistry, 2006, 106, 2597-2602.	2.0	3
116	Polaron stability under collision with different defects in conjugated polymers. International Journal of Quantum Chemistry, 2006, 106, 2603-2608.	2.0	5
117	Fitting potential energy surface of reactive systems via genetic algorithm. International Journal of Quantum Chemistry, 2006, 106, 2650-2657.	2.0	14
118	Thionin adsorption on silicon (1 0 0): Structural analysis. Applied Surface Science, 2006, 253, 1978-1982	2.6.1	4
119	Investigation of surface passivation process on magnetic nanoparticles by Raman spectroscopy. Surface Science, 2006, 600, 3642-3645.	1.9	21
120	Optical signatures of asymmetric fractal diffusion of electron-hole plasma in semiconductor quantum wells. Applied Physics Letters, 2006, 89, 142103.	3.3	3
121	Investigation of the interaction between magnetic nanoparticles surface-coated with carboxymethyldextran and blood cells using Raman spectroscopy. Journal of Magnetism and Magnetic Materials, 2005, 289, 452-454.	2.3	6
122	Optical and transport properties of InAs/GaAs quantum dots emitting at 1.314m. Microelectronics Journal, 2005, 36, 194-196.	2.0	1
123	Surface passivation and characterization of cobalt–ferrite nanoparticles. Surface Science, 2005, 575, 12-16.	1.9	13
124	Raman study of nanoparticle-template interaction in a CoFe2O4/SiO2-based nanocomposite prepared by sol–gel method. Journal of Magnetism and Magnetic Materials, 2005, 289, 139-141.	2.3	39
125	Structural phases of coupled polyacetylene chains with impurities. International Journal of Quantum Chemistry, 2005, 103, 597-603.	2.0	1
126	Quantum-controlled NOT gate made of coupled polyacetylene chains. International Journal of Quantum Chemistry, 2005, 103, 543-549.	2.0	1

#	Article	IF	CITATIONS
127	Dynamic interaction between polarons and torsional vibrations in conjugated polymers. International Journal of Quantum Chemistry, 2005, 103, 604-609.	2.0	4
128	In vitro investigation of mice blood doped with magnetite-coated nanoparticles. , 2005, , .		0
129	Structural stability study of cobalt ferrite-based nanoparticle using micro Raman spectroscopy. Journal of Magnetism and Magnetic Materials, 2004, 272-276, 2357-2358.	2.3	52
130	Carrier diffusion in InGaAs/GaAs quantum wells grown on vicinal substrates. Physica E: Low-Dimensional Systems and Nanostructures, 2004, 23, 466-470.	2.7	3
131	Indications of amplified spontaneous emission in the energy transfer between InAs self-assembled quantum dots. Physical Review B, 2004, 70, .	3.2	14
132	Stability of citrate-coated magnetite and cobalt-ferrite nanoparticles under laser irradiation: A raman spectroscopy investigation. IEEE Transactions on Magnetics, 2003, 39, 2645-2647.	2.1	70
133	Coupled rate equation modeling of self-assembled quantum dot photoluminescence. Microelectronics Journal, 2003, 34, 705-707.	2.0	1
134	CW photoluminescence determination of the capture cross-section of self-assembled InAs quantum dots. Physica E: Low-Dimensional Systems and Nanostructures, 2003, 17, 107-108.	2.7	2
135	Asymmetric carrier transport in InGaAs quantum wells and wires grown on tilted InP substrates. Physica E: Low-Dimensional Systems and Nanostructures, 2003, 17, 169-171.	2.7	2
136	Observation of the spectral dependence of the spatial photocarrier redistribution in InAs/GaAs quantum dots. Physica E: Low-Dimensional Systems and Nanostructures, 2003, 17, 120-121.	2.7	0
137	Photoexcited carrier diffusion in self-assembled InAs/GaAs quantum dots with different dot densities. Physica E: Low-Dimensional Systems and Nanostructures, 2003, 17, 122-123.	2.7	2
138	Dynamics of polarons and bipolarons with interchain coupling in conjugated polymers. International Journal of Quantum Chemistry, 2003, 95, 153-158.	2.0	10
139	Polyacetylene as a qubit system. International Journal of Quantum Chemistry, 2003, 95, 224-229.	2.0	1
140	Time-resolved measurements and spatial photoluminescence distribution in InAs/AlGaAs quantum dots. Microelectronics Journal, 2003, 34, 747-749.	2.0	4
141	Carrier kinetics in quantum dots through continuous wave photoluminescence modeling: A systematic study on a sample with surface dot density gradient. Journal of Applied Physics, 2003, 94, 1787-1794.	2.5	15
142	Experimental evidence of asymmetric carrier transport in InGaAs quantum wells and wires grown on tilted InP substrates. Applied Physics Letters, 2002, 81, 2460-2462.	3.3	7
143	Investigation of optical and structural properties of InxGa1â^'xAs/GaAs quantum wells grown on vicinal GaAs(001) substrates. Physica B: Condensed Matter, 2002, 311, 285-291.	2.7	2
144	Raman spectroscopy of magnetoliposomes. Journal of Magnetism and Magnetic Materials, 2002, 252, 415-417.	2.3	9

#	Article	IF	CITATIONS
145	Raman spectroscopy in magnetic fluids. New Biotechnology, 2001, 17, 41-49.	2.7	28
146	Step-Bunching Evidence in Strained InxGa1?xAs/GaAs Quantum Wells Grown on Vicinal (001) Substrates. Physica Status Solidi A, 2001, 187, 253-256.	1.7	1
147	Excitation Transfer through Quantum Dots Measured by Microluminescence: Dependence on the Quantum Dot Density. Physica Status Solidi A, 2001, 187, 45-48.	1.7	5
148	Study of the interactions between the surface chemisorbed layer and the surrounding media in magnetite-coated nanoparticles using Raman spectroscopy. Journal of Magnetism and Magnetic Materials, 2001, 226-230, 1890-1892.	2.3	3
149	Asymmetric carrier diffusion and phonon-wind-driven transport in an InGaAs-InP quantum well. Springer Proceedings in Physics, 2001, , 815-816.	0.2	0
150	Symmetric and asymmetric fractal diffusion of electron–hole plasmas in semiconductor quantum wells. Physics Letters, Section A: General, Atomic and Solid State Physics, 2000, 268, 430-435.	2.1	12
151	Phonon-wind-based transport in InGaAs-InP quantum well under intense optical excitation. Physical Review B, 2000, 62, 6924-6927.	3.2	12
152	Raman spectroscopy in oleoylsarcosine-coated magnetic fluids: a surface grafting investigation. IEEE Transactions on Magnetics, 2000, 36, 3712-3714.	2.1	5
153	Raman Investigation of Uncoated and Coated Magnetic Fluids. Journal of Physical Chemistry A, 2000, 104, 2894-2896.	2.5	24
154	Ambipolar carrier diffusion in In0.53Ga0.47As single quantum wells. Brazilian Journal of Physics, 1999, 29, 690-693.	1.4	0
155	Spatial and temperature dependence of carrier recombination in an InGaAs/InP heterostructure. Journal of Applied Physics, 1999, 85, 2866-2869.	2.5	18
156	Defect-limited carrier diffusion in In0.53Ga0.47As-InP single quantum well. Physica B: Condensed Matter, 1999, 273-274, 963-966.	2.7	7
157	Raman study of ionic water-based copper and zinc ferrite magnetic fluids. Journal of Magnetism and Magnetic Materials, 1999, 201, 105-109.	2.3	30
158	Investigating charge transport in molecular switches with neural networks. Journal of Computational Chemistry, 1999, 20, 1060-1066.	3.3	5
159	Fano-like electron–phonon interference in δ-doping GaAs superlattices. Superlattices and Microstructures, 1998, 23, 1033-1035.	3.1	0
160	Raman study of interface modes subjected to strain in InAs/GaAs self-assembled quantum dots. Physical Review B, 1998, 58, R1770-R1773.	3.2	50
161	Surface phonon observed in GaAs wire crystals grown on porous Si. Journal of Physics Condensed Matter, 1998, 10, 9687-9690.	1.8	15
162	Photoluminescence study of spin - orbit-split bound electron states in self-assembled InAs and quantum dots. Journal of Physics Condensed Matter, 1997, 9, L13-L17.	1.8	7

#	Article	IF	CITATIONS
163	Characterization of GaAs wire crystals grown on porous silicon by Raman scattering. Journal of Applied Physics, 1997, 82, 6247-6250.	2.5	18
164	Photoluminescence of Excitons in Differently Oriented Self-Assembled InAs Quantum Dots. Physica Status Solidi A, 1997, 164, 455-457.	1.7	2
165	Raman study of Fano-like electron-phonon coupling in δ-doping GaAs superlattices. Physical Review B, 1996, 54, 13927-13931.	3.2	8
166	Raman study of interface roughness in(GaAs)n(AlAs)nsuperlattices grown on tilted surfaces: Evidence of corrugation of the (113) interface. Physical Review B, 1996, 53, 1927-1932.	3.2	12
167	Optical phonon spectra of GaSb/AlSb superlattices: Influence of strain and interface roughnesses. Journal of Applied Physics, 1996, 80, 597-599.	2.5	7
168	Comparative Raman studies of cubic and hexagonal GaN epitaxial layers. Journal of Applied Physics, 1996, 79, 4137.	2.5	85
169	Atomic-scale characterization of interfaces in the GaAs/AlGaAs superlattices. Materials Science and Engineering B: Solid-State Materials for Advanced Technology, 1995, 35, 180-183.	3.5	1
170	Influence of atomic-scale roughness on Raman selection rules in the ultrathin-layer (GaAs)n1(AlAs)n2superlattices. Physical Review B, 1995, 51, 9891-9894.	3.2	8
171	Raman scattering of the optical vibrational modes in (GaAs)n(AlAs)nsuperlattices grown on (311)Aand (311)Bsurfaces. Physical Review B, 1995, 51, 5473-5476.	3.2	10
172	Spectroscopy of the optical vibrational modes in GaAs/AlxGa1â^'xAs heterostructures with monolayer-wideAlxGa1â^'xAs barriers. Physical Review B, 1995, 52, 2610-2618.	3.2	19
173	Crystallization process of amorphous GaSb films studied by Raman spectroscopy. Journal of Applied Physics, 1995, 77, 4044-4048.	2.5	24
174	Optical stability of citrate-coated magnetite and cobalt-ferrite nanoparticles: a Raman spectroscopy investigation. , 0, , .		0
175	STRUCTURAL CHARACTERIZATION OF Co-DOPED ZnO NANOPARTICLES USING X-RAY DIFFRACTION AND RAMAN SPECTROSCOPY. , 0, , .		Ο